ISSN 1547-4771, Physics of Particles and Nuclei Letters, 2013, Vol. 10, No. 6, pp. 587–596. © Pleiades Publishing, Ltd., 2013.

RADIOBIOLOGY, ECOLOGY AND NUCLEAR MEDICINE

A Quantitative Model of Bacterial Mismatch Repair as Applied to Studying Induced Mutagenesis[1]

O. V. Belov[a], O. Chuluunbaatar[a, b], M. I. Kapralov[a], and N. H. Sweilam[c]

[a] *Joint Institute for Nuclear Research, Dubna*

[b] *School of Mathematics and Computer Science, National University of Mongolia, Ulaanbaatar*

[c] *Mathematics Department, Faculty of Science, Cairo University, Giza, Egypt*

e-mail: chuka@jinr.ru; nsweilam@sci.cu.edu.eg

Abstract—The paper presents a mathematical model of the DNA mismatch repair system in *Escherichia coli* bacterial cells. The key pathways of this repair mechanism were simulated on the basis of modern experimental data. We have modelled in detail five main pathways of DNA misincorporation removal with different DNA exonucleases. Here we demonstrate an application of the model to problems of radiation-induced mutagenesis.

DOI: 10.1134/S1547477113060046

INTRODUCTION

The methyl-directed mismatch repair (MMR) is one of the biological systems capable of correcting the noncomplementary nucleotide pairs that appear as a consequence of certain factors [1, 2]. This repair system was identified in many organisms including bacteria, yeasts, and mammals. The biochemical mechanisms of MMR are quite conservative in relation to different organisms. However, the interrelations of its pathways and other repair systems are well understood only for relatively simple biological objects like prokaryotic cells.

The MMR system can be started by many factors including the errors that occur during normal DNA replication and cell metabolism as well as a spectrum of DNA lesions induced by exposure to different agents of physical and chemical nature and the following DNA repair processes [3]. Among the physical factors capable of inducing this system, the action of radiations of different types is very interesting in terms of its use as an instrument for studying the MMR connections with other repair systems responsible for the mutagenic effects in the living organisms. There are a number of experimental observations supporting the possible role of MMR in the mutagenic effects of different types of radiations [4, 5]. Some of these findings suggest the involvement of MMR in mutagenic pathways of other repair systems.

Many-year studies identified an important role of the SOS repair in mutagenesis induced by different types of radiation [6–8]. It was shown, that a key role in SOS network belongs to PolV Mut protein complex comprising DNA polymerase V (or $UmuD'_2C$). This specific polymerase is able to process DNA synthesis through the lesions which were not removed by earlier repair stages [9]. This mechanism called translesion synthesis (TLS) is also realized in mammalian and human cells [10, 11].

As is known, PolV Mut demonstrates a relatively high error frequency during the incorporation of bases in nascent strands opposite DNA lesions [12]. However, the finally measured mutation frequency in individual genes is not so high as it might have been if all errors produced by the PolV Mut complex had been ixed as mutations. Our previous research related to the mathematical modelling of the mechanism of SOS-induced mutagenesis under 254 nm ultraviolet (UV) radiation demonstrated this fact by an interval of the free parameter value responsible for fixing the PolV-induced errors as mutations [13]. These conclusions made us introduce in our model additional repair mechanisms at the final stages of SOS response. Taking into account the specific character of DNA synthesis by the PolV Mut complex and relying on the corresponding experimental facts, we have chosen the MMR system of *E. coli* bacterial cells for the theoretical analysis of its influence on the UV-induced mutagenic effect.

1. THEORY

1.1. The Mechanism of MMR

Studies of the MMR system of bacterial cells have allowed finding out the role of the main proteins in the regulation of its functions. The results of modern experiments as regards the description of the biochemical steps that follow MMR activation can be generalized as a scheme in Fig. 1.

[1] The article is published in the original.

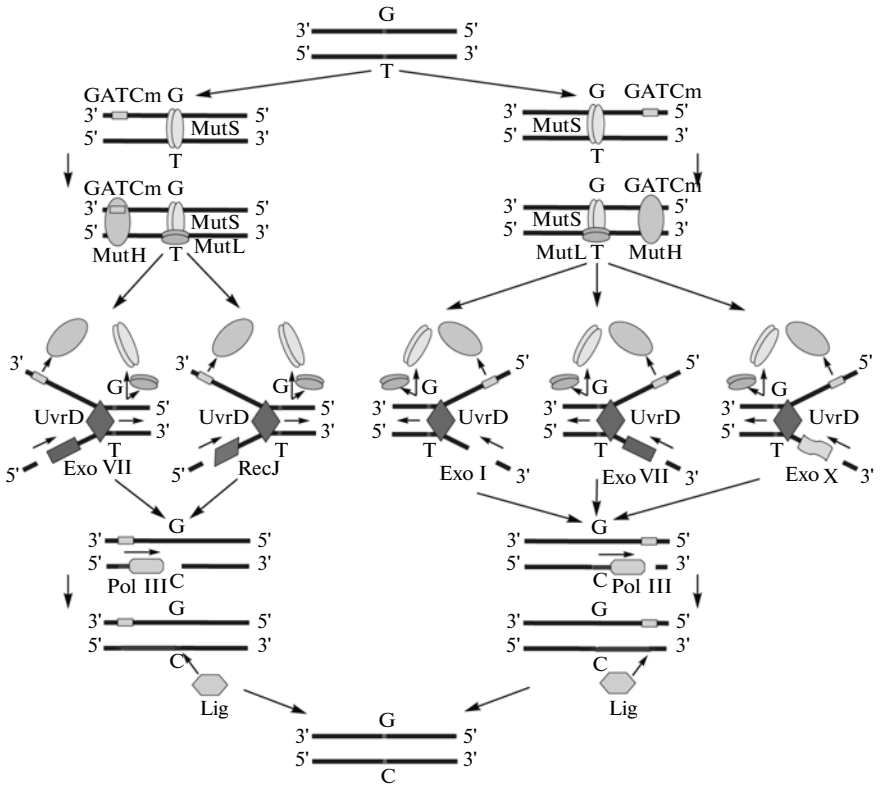

Fig. 1. Scheme of the *MMR* mechanism in *E. coli* bacterial cells (explanation in the text).

After the appearance of misincorporated nucleotides in the DNA chain, *E. coli's* MMR system detects the mismatch shortly after the DNA replication round ends. The way to detect an incorrect base on the newly synthesized strand is based on the process of DNA methylation, which does not occur until several minutes after the strand is produced. This mechanism provides a distinction between the parental strand, which is already methylated, and the daughter strand containing an error [1, 14]. The recognition of a wrongly incorporated nucleotide is performed by the MutS protein, which binds to the site with a mismatch as a homodimer and forms a complex with the MutL protein. Interaction with MutL enhances mismatch recognition, and recruits MutH protein to the region. MutL also functions as a homodimer—in contrast with MutH, which acts as a monomer [3]. MutH finds a hemi-methylated dGATC sequence and joins the unmethylated DNA strand. Then the $MutS_2L_2$ complex activates the MutH protein in the presence of ATP. During this interaction, MutH makes a strand-specific nick that can occur either 3' or 5' to the mispair on the unmethylated strand. In the presence of MutL, helicase II (or UvrD) loads at the nicked site and unwinds the nascent strand [15]. The single-stranded DNA (ssDNA) produced in this process is bound by the single-strand binding protein (SSB), which protects ssDNA from a nuclease attack. Further MMR steps require the activity of four exonucleases: ExoI, ExoVII, ExoX, and RecJ encoded by the *xonA, xseA, exoX*, and *recJ* genes, respectively. These exonucleases are able to digest the nonmethylated strand from the dGATC nicked site to just beyond the mismatch. This excision process could proceed either from 5' to 3' or from 3' to 5' end to the mispair [3]. ExoI and ExoX digest the DNA strand in the 3' to 5' direction, RecJ degrades it from 5' to 3', and ExoVII can excise DNA in both directions [16]. The resulting single-stranded gap is filled by DNA polymerase III holoenzyme (PoIIII) with SSB. The remaining DNA strand is joined to existing one by the DNA ligase [2].

1.2. MMR and SOS Response

Recently, a number of experimental facts allowed formulating the hypothesis that the MMR system significantly reduces the error rates during DNA replication by recognizing and correcting mismatches which prevent normal replication [17]. It was also found that MMR can process the incorrect bases opposite UV-induced photoproducts which were not removed by early repair processes like photoreactivation or nucleotide excision repair and during SOS response [4]. Summarizing all these facts, we can conclude that the main way of the interaction between the inducible SOS system and MMR is the methyl-directed excision of incorrect bases inserted by PolV Mut in nascent

strands during translesion synthesis. Under the induction of SOS response, the amount of the misincorporated bases, which are the substrate for MMR, becomes much higher than under normal conditions when MMR repairs mainly spontaneously induced lesions. Within our model approach we show how the interactions between these two systems could be realized taking into account the modern data on the biochemical mechanisms of the MMR and SOS systems.

2. MATHEMATICAL MODEL

In our previous study, we developed a mathematical model of *E. coli's* mutation process induced by UV radiation [13, 18, 19]. Using this model, we analysed the chain of events from primary DNA lesion appearance to fixing this lesion as a mutation. We also described quantitatively the relationships between the biochemical processes realized during the SOS response and translesion synthesis effectiveness. It was shown how this model could be applied for the estimation of the mutagenic effect of UV radiation. We demonstrated this ability of our model by estimating the mutation frequency in *E. coli's lacI* gene. To describe the relationships between SOS response and MMR, we combine the model developed earlier with a newly designed mathematical approach to methyl-directed repair.

To design a model of MMR, we have simulated the dynamical changes of the concentrations of MMR proteins and intermediate complexes concentrations using reversible mass-action kinetics. The reaction network, which highlights mass transfer and regulatory reactions, is presented in Fig. 2.

In the general view, the equations of the model could be expressed as follows:

$$\frac{dX_i}{dt} = V_{i+}(X_i, X_0) - V_{i-}(X_i, X_0), \qquad (1)$$

where X_i ($i = 1, ..., n$) is the ith regulatory protein intracellular concentration; X_0 is an inducing signal which represents the amount of the nucleotides misincorporated by the PolV Mut complex, and t is the time. The functions V_{i+} and V_{i-} describe the ith protein accumulation and degradation, respectively.

For our model, we singled out five MMR pathways with four exonucleases taking into account their ability to digest a nascent DNA strand in different polarity. The dimensionless equations for each protein and intermediate complexes of the MMR system as well as their initial conditions are given in Appendix A (Eqs. (A.1)) in a compact form. We divided the total yield of errors produced by the PolV Mut complex into five subyields $X_{00,n}$ ($n = 1, ..., 5$) which possess the corresponding 3' or 5' polarity depending on the position of the MutH-mediated nick and therefore should be repaired with different exonucleases. $X_{00,1}$ represents the mispairs with 3' nick to their position to be repaired by the ExoI pathway; $X_{00,2}$ and $X_{00,3}$ are the subyields with 3' and 5' nicks to the mismatch, respectively, to be processed with ExoVII; $X_{00,4}$ and $X_{00,5}$ represent the yields with 3' and 5' nicks to be repaired by ExoX and RecJ pathways, respectively. In this study, we assume that 3' and 5' MutH-mediated nicks as well as the involvement of exonucleases possessing the same end specificity are equally probable.

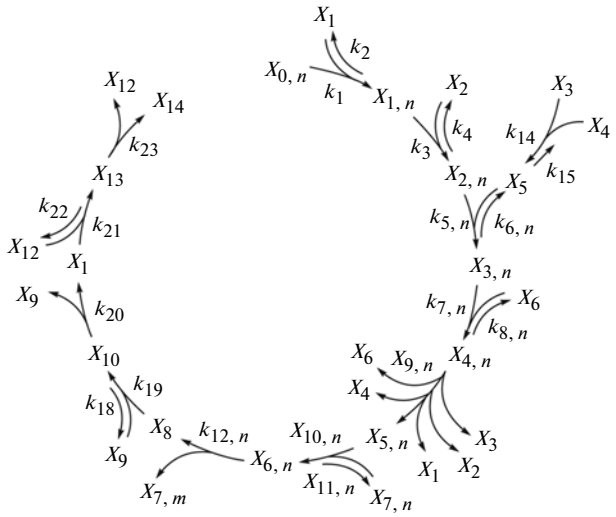

Fig. 2. Scheme representing the *MMR* reaction network used in the model. Here $X_{0,n}$, X_1, X_2, X_3, X_4, X_6, $X_{7,m}$, X_9, X_{12}, and X_{14} are the concentrations of mismatches—$MutS_2$, $MutL_2$, MutH, GATCm, UvrD, exonucleases of the m type, PolIII, DNA ligase, and repaired DNA, respectively; $X_{1,n}$, $X_{2,n}$, $X_{3,n}$, $X_{4,n}$, $X_{5,n}$, $X_{6,n}$, X_8, X_{10}, X_{11}, and X_{13} are the intermediates formed during repair. The synthesis and nonspecific losses of the *MMR* proteins are omitted.

Most genes encoding the main MMR proteins in *E. coli* cells are SOS-independent, i.e., their synthesis is not controlled by the LexA protein. But the expression of the *UvrD* gene producing helicase II strongly depends on the intracellular concentration of the LexA repressor [20, 21]. To describe the regulation of the UvrD transcription by the LexA protein, we used the model of gene regulation used in many papers [13, 22, 23]. The irst term in the equation for the UvrD helicase (Eqs. (A.1)) describes LexA-regulated synthesis. The dimensional expression for the UvrD protein synthesis is the following:

$$V_{6,\,\mathrm{sint}} = \frac{kX_{06}(1 + (X_{0L}/\gamma)^h)}{1 + (X_L/\gamma)^h}. \qquad (2)$$

Here X_{06} and X_{0L} are the dimensional initial concentrations of the UvrD helicase and LexA protein; γ is the dissociation rate constant of the LexA monomer from the *UvrD* gene operator; h is the Hill coefficient characterizing LexA binding cooperativity; X_L is the

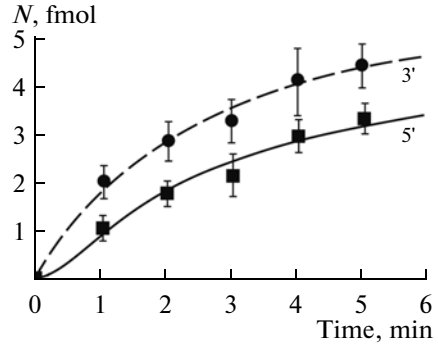

Fig. 3. Incision of a 3' (●) and 5' (■) hemimethylated heteroduplexes by activated MutH in the presence of MutS and MutL. *N* is the concentration of incised DNA. The curves are the calculated results; the dots are the experimental data [27].

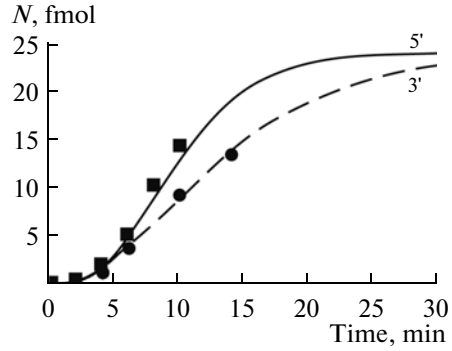

Fig. 4. Excision of a nicked 3' (●) and 5' (■) heteroduplexes by activated ExoI (3') and RecJ (5') in the presence of MutS, MutL, DNA helicase II, and *SSB*. *N* is the concentration of excised DNA. The curves are the calculated results; the dots are the experimental data [27].

current intracellular LexA concentration, and k is the kinetic rate constant.

The values of the kinetic rate constants are defined using values measured experimentally and by fitting the model to existing experimental data on the MMR kinetics at different stages of repair. The full set of model parameters and their normalization are described in Appendix B.

To calculate $X_{00,1}$, $X_{00,2}$, $X_{00,3}$, $X_{00,4}$, and $X_{00,5}$ we used our translesion synthesis model developed earlier [13]. It describes illing of single strand DNA gaps opposite thymine dimers by the PolV Mut complex and calculates the mean value of the errors produced by this complex depending on time and energy fluence of UV radiation. The input data for this model is the kinetics of the UmuD'$_2$C complex calculated in our previous study for UV energy fluences up to 100 J/m^2. In our model $X_{00,1}$, $X_{00,2}$, $X_{00,3}$, $X_{00,4}$, and $X_{00,5}$ are directly proportional to previously calculated mean number of errors. Taking into account the equiprobability of launching all the five subpathways, we set these subyields equal to 1/5 of the error value.

Our model allows describing the mutation process in individual genes. The dependence of the mutation frequency on the UV energy fluence is described by the following expression [8, 13]:

$$\frac{Z_m}{Z(\Psi)} = \theta_1\Psi + \theta_2\Psi(1 - \exp(-\theta_3\Psi)), \qquad (3)$$

where Z_m and Z are the numbers of the mutants and survived cells, respectively; Ψ is the UV energy fluence; $\theta_1\Psi$ is the linear component of the dependence; $\theta_2\Psi$ is proportional to mutation yield; and $(1 - \exp(-\theta_3\Psi))$ is the fraction of mutations induced by mutagenic repair.

In this paper, we have estimated the mutation frequency not only for bacterial strains with the normal functioning of the MMR and SOS systems (*mut*$^+$ and *umu*$^+$ bacteria) but also for mutant strains carrying defects in the *mutS, mutL, mutH* (*mut*$^-$) and *umuC* genes (*umu*$^-$). As a rule, the *mut*$^-$ bacteria demonstrate a spontaneous level of mutagenesis. Therefore, to describe the mutation frequency in these strains, we need to introduce a parameter θ_0 characterizing spontaneous mutagenesis in Eq. (3):

$$\frac{Z_m}{Z(\Psi)} = \theta_0 + \theta_1\Psi + \theta_2\Psi(1 - \exp(-\theta_3\Psi)). \qquad (4)$$

This parameter, which is an input parameter of the model, does not depend on the UV energy fluence and can be specified on the basis of experimental data. For the strains with the normal genotype, $\theta_0 = 0$ because the mutation frequency for these strains is negligible without irradiation [4]. The experimental values of θ_0 and θ_1 as well as the procedure of evaluating the parameters θ_2 and θ_3 are given in Appendix B.

For the *umu*$^-$ bacteria defective in the functioning of the SOS system, we need to put $\theta_3 = 0$ because the share of cells with induced SOS response will be zero. Therefore, the mutation frequency will depend only on spontaneous mutagenesis and on the linear component characterizing the mutagenic lesions that are ixed during constitutive repair or during DNA replication.

3. RESULTS

The results of the parameter fitting procedure show an adequate set of parameters for the developed model (Figs. 3–5). The calculated curves reconstruct the kinetics of different in vitro MMR stages well. This fact enables us to use our model for the identification of intracellular mechanisms realizing the connections between mutagenic SOS response and methyl-directed mismatch repair. The developed model allows a comprehensive quantitative analysis of protein–protein interactions within the molecular networks of these two systems. We do not show here detailed data calculated for the dynamical change of MMR protein

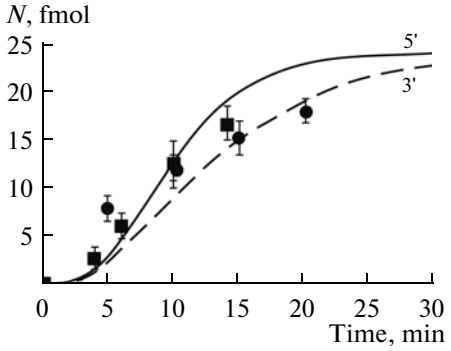

Fig. 5. Single-stranded gap filling of an excised 3' (●) and 5' (■) heteroduplexes by PolIII in the presence of MutS, MutL, DNA helicase II, ExoI or RecJ, and *SSB*. *N* is the concentration of rebuilt DNA. The curves are the calculated results; the dots are the experimental data [27].

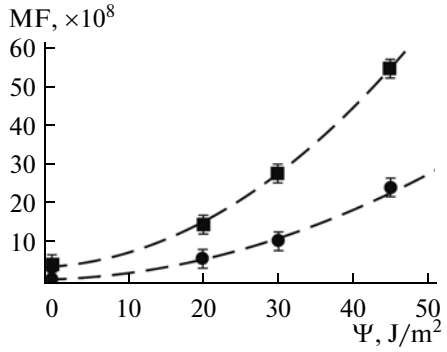

Fig. 6. Dependence of the mutation frequency on UV energy fluence calculated for mut^+ (the solid line) and $mutS^-$ (the dashed line) strains. The symbols represent experimental data for mut^+ (●) and $mutS^-$ (●) strains [4]. The experimental data with their standard errors of the means ($\times 10^{-8}$) for mut^+ and *mutS* are, respectively, 0 J/m^2, 0, 4.0 ± 0.4; 20 J/m^2, 14.4 ± 0.9, 5.7 ± 0.2;30 J/m^2, 28.0 ± 3.4, 10.2 ± 0.9; 45 J/m^2, 55.0 ± 1.0, 24.4 ± 4.2.

concentrations because the main aim of this paper is to demonstrate the effect of the mismatch repair on radiation-induced SOS mutagenesis.

3.1. Mutagenesis in Bacteria Defective in MMR Functions

Using our model we have performed calculations of the mutation frequency in *E. coli* strains with different genotypes. The mutagenic effect of UV radiation was modeled for cells with normal SOS and MMR functions and for three types of mutants defective in the *mutS, mutL*, or *mutH* gene. In this study, we have estimated the mutation frequency in the *E. coli's lacZ* gene encoding β-galactosidase. The computation procedure consisted in running simultaneously the models for SOS-induced mutagenesis, translesion synthesis, and the MMR system with the corresponding set of parameters responsible for the inhibition of MutS, MutL, or MutH protein functions (i.e., the parameters X_{01}, X_{02}, or X_{03} were assumed to be zero). Figure 6 shows the results calculated for the mut^+ and $mutS^-$ strains in comparison with experimental data on the revertant frequency in two alleles at *lacZ* codon 461, which reverts via CCC → CTC and CTT → CTC transitions [4]. We assume that these measured data reflect the general pattern of the mutagenic response of *E. coli* cells to UV radiation. In our calculations, we have obtained the 2.6-fold averaged increase in the mutation frequency in a $mutS^-$ strain as compared with a mut^+ one. This value is the same as in experiment mentioned above. At $\Psi = 0$ J/m^2, the curve computed for the $mutS^-$ strain starts from the averaged spontaneous level of mutagenesis equalling to 4×10^{-8}. For these two cases, our calculations give the following values of the parameter $P(X)$: 6.1×10^{-8} for mut^+ and 1.6×10^{-7} for $mutS^-$. The consideration of the MMR mechanism introduced into the model description of SOS-induced mutagenesis slightly changes the sense of this parameter. We indicated before that this parameter reflects the error probability during nucleotide pasting by PolV Mut on DNA sites which do not contain thymine dimers. But a more detailed understanding of the mechanisms behind $P(X)$ provides a new explanation of its meaning. It could be interpreted as the resulting probability of the error fixation after DNA resynthesis by the PolV Mut complex. It means that $P(X)$ reflects not only error induction by PolV Mut but the probability of mutation appearance at the place of a wrongly inserted nucleotide. That is the main reason why the new values of this parameter are much lower than the ones obtained before [13]. Another fact that underlies the lower $P(X)$ values is that the average error rate of PolV during the replication of undamaged DNA is ~10^{-4} [24], but the resulting mutation frequency is much lower than it could be if all ssDNA gaps would be illed by this polymerase without any mechanism reducing its mutagenic activity.

We have also calculated the mutation frequency for $mutL^-$ and $mutH^-$ bacteria at a single UV energy fluence of 30 J/m^2 (Fig. 7). The obtained results for these strains are about two times higher than for mut^+ ones just like in the experiment [4]. The $P(X)$ parameter values for these cases are given in Appendix B. Taking into account the experimental standard errors of means (SEM), we can conclude that the model adequately reconstructs the observed mutagenic effect.

3.2. Mutagenesis in Bacteria Defective in SOS and MMR Functions

As is known, a defect in some of *umuDC* genes leads to the inactivation of the SOS function because it prevents the normal assembling of UmuD'$_2$C complex, which is the main component of PolV Mut. In our

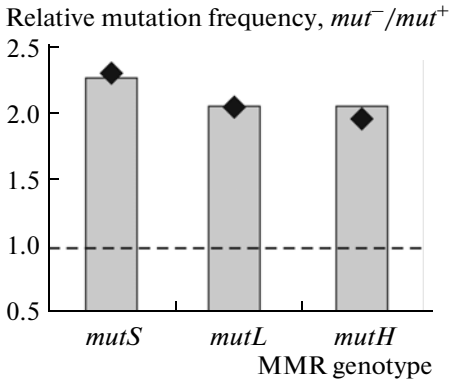

Fig. 7. Mutation frequency in bacteria defective in the *mutL* and *mutH* functions at the UV energy fluence of 30 J/m^2.

model, we reconstructed the mutagenic effect observed experimentally under the defect in *umuC* gene and violations in the *mutS, mutL*, and *mutH* functions of MMR systems. Setting the parameter θ_0 according to the average spontaneous mutation frequency for *umu*$^-$ *mut*$^-$ strains, we calculated the level of mutagenesis to be $\sim 5.7 \times 10^{-8}$ which is close to experimental data [4]. As for *umu*$^+$*mut*$^-$ bacteria, the computation procedure included running three models together with the initial conditions reflecting the corresponding genotype, i.e., X_{01}, X_{02}, X_{03}, and the initial concentration of UmuC in the SOS-mutagenesis model were zero.

DISCUSSION

Our model accentuates the role of the MMR system in radiation-induced SOS mutagenesis. Choosing UV radiation as a mutagenic factor for this study is explained by the necessity to indicate the links between MMR and SOS response without any significant influence of other repair systems such as single- and double-strand break repair and base excision repair. Since most of the UV-induced DNA lesions represent a substrate for SOS repair, it gives an opportunity to identify the direct connections between the biochemical mechanisms of these two systems. The developed models provide a topological view of the MMR and SOS networks, which is another way to clarify their biological relations. The precise modelling of enzymatic mechanisms together with the mathematical description of mutagenic effects brings a specific insight into the problem of induced mutagenesis, opening up a possibility of exploring the effects of different molecular mechanisms on the final mutagenic reaction of the living organism. In this paper, we have shown how more or fewer functions connected with the activity of the *mutS, mutL, mutH*, and *umuC* genes affect the mutation frequency, i.e., what influence the system's different topologies have on the final cell response to irradiation. It was proved theoretically that a violation of the expression of one of these genes leads to an increase in mutagenesis in bacterial cells. It is clear that this fact could be extrapolated to other SOS genes responsible for assembling the PolV Mut complex. According to our model, violations in the *umuD* or *recA* gene result in the same mutation frequency as in *umuC*-defective strains.

Besides our previous studies, only a few studies are concerned with simulating some quantitative characteristics of TLS [25, 26]. However, these approaches do not provide a system view of the process as well as do not focus on its probabilistic aspects and connections with other repair systems. One of the main features of our models is a clear representation of cause-and-effect relations between two complicate repair networks and the TLS effectiveness.

Considering our models, one might think that the quantitative estimation of mutagenic effects can be done with a much simpler analysis than the development of a complicated mathematical model to compute parameters in the classical equation for the mutation frequency. However, such a simplified approach gives no information as to which biophysical processes are behind these parameters. The models similar to ours clearly indicate the dependence of parameter values on real biological mechanisms. This justifies the claim to novelty and makes these models useful. Taking into account the knowledge of the molecular mechanisms of other *E. coli's* repair systems, it could be suggested that the MMR system plays a role in SOS mutagenesis induced not only by UV radiation but also by ionizing radiations of different quality. The latter relates mostly to the repair of clustered DNA lesions formed after irradiation by charged particles because it is supposed that these lesions make up the main substrate for mutagenic SOS repair.

APPENDICES

Appendix A

THE SYSTEM OF DIFFERENTIAL EQUATIONS

Equations (A.1) represent a compact form of the system of ordinary differential equations describing MMR pathways. Here $y_{0,n}$ are the normalized intracellular concentrations of the mismatches (Mism$_n$) produced by the PolV Mut complex which will be repaired by n different pathways. The y_1 is the concentration of the MutS dimer, which recognizes a mismatch and binds to it reversibly forming an intermediate Mism$_n$MutS$_2$ complex ($y_{1,n}$). The y_2 represents the normalized concentration of the MutL dimer, which joins the Mism$_n$MutS$_2$ complex and forms the next intermediate Mism$_n$MutS$_2$MutL$_2$ ($y_{2,n}$). The y_3 is the concentration of the MutH protein interacting with the methylated GATCm sequence (y_4) with the pro-

duction of the GATCmMutH complex (y_5). The $y_{3,n}$ are the concentrations of nicked DNA after the interaction of $\mathrm{Mism}_n\mathrm{MutS}_2\mathrm{MutL}_2$ complexes with GATCmMutH. The molecules of the MutS_2, MutL_2, and MutH proteins remain joined to the nicked DNA strand. The following strand unwinding by the UVrD-helicase (y_6) can be represented as a typical enzymatic reaction with the intermediate complex $y_{4,n}$ and resulting detachment of MutS_2, MutL_2, MutH, and UvrD. Since the synthesis of the UvrD helicase is SOS-dependent, we introduced the normalized concentration of the LexA protein (y_L) into the equation for y_6. The kinetics of LexA is calculated using the model of SOS-induced mutagenesis [13]. The action of UvrD leads to the formation of an unwound DNA site $y_{5,n}$ which will be processed by five pathways with four exonucleases $y_{7,m}$ ($m = 1, ..., 4$ for ExoI, ExoVII, ExoX, and RecJ, respectively). The first pathway ($n = 1$) is related to 3'-nicked DNA excision by ExoI; the second and third ones ($n = 2$ and $n = 3$) describe, respectively, 3'-and 5'-nicked strand excision by ExoVII. When $n = 4$, the 3'-nicked strand is cut out by ExoX; and for $n = 5$, 5'-nicked DNA excision is processed by RecJ. In our model, these interactions are also presented as enzymatic reactions with intermediate complexes between a nicked strand and the corresponding exonuclease ($y_{6,n}$) and the formation of a single-strand DNA gap (y_8). The y_9 is the normalized concentration of PolIII. The y_{10} describes the amount of the intermediate complex representing PolIII molecules bound to a single-strand gap during DNA resynthesis. The y_{11} is the concentration of the newly synthesized DNA sequence with two small gaps at its edges. The last MMR stage is characterized in the model by a reaction describing the ligation of a new sequence by a DNA ligase (y_{12}),where y_{13} is the intermediate complex and y_{14} is repaired DNA;

$$\frac{dy_{0,n}}{d\tau} = p_2 y_{1,n} - p_1 y_1 y_{0,n},$$

$$\frac{dy_{1,n}}{d\tau} = p_1 y_1 y_{0,n} + p_4 y_{2,n} - y_{1,n}(p_2 + p_3 y_2),$$

$$\frac{dy_{2,n}}{d\tau} = p_3 y_2 y_{1,n} + p_{6,n} y_{3,n} - y_{2,n}(p_4 + p_{5,n} y_5),$$

$$\frac{dy_{3,n}}{d\tau} = p_{5,n} y_5 y_{2,n} + p_{8,n} y_{4,n} - y_{3,n}(p_{6,n} + p_{7,n} y_6),$$

$$\frac{dy_{4,n}}{d\tau} = p_{7,n} y_6 y_{3,n} - y_{4,n}(p_{8,n} + p_{9,n}),$$

$$\frac{dy_{5,n}}{d\tau} = p_{9,n} y_{4,n} + p_{11,n} y_{6,n} - p_{10,n} y_{7,m} y_{5,n},$$

$$\frac{dy_{6,n}}{d\tau} = p_{10,n} y_{7,m} y_{5,n} - y_{6,n}(p_{11,n} + p_{12,n}),$$

$$\frac{dy_1}{d\tau} = y_{01} + p_2 \sum_{n=1}^{5} y_{1,n} + \sum_{n=1}^{5} p_{9,n} y_{4,n} - y_1\left(p_1 \sum_{n=1}^{5} y_{0,n} + p_{13}\right),$$

$$\frac{dy_2}{d\tau} = y_{02} + p_4 \sum_{n=1}^{5} y_{2,n} + \sum_{n=1}^{5} p_{9,n} y_{4,n} - y_2\left(p_3 \sum_{n=1}^{5} y_{1,n} + p_{13}\right),$$

$$\frac{dy_3}{d\tau} = y_{03} + \sum_{n=1}^{5} p_{9,n} y_{4,n} + p_{15} y_5 - y_3(p_{14} y_4 + p_{13}),$$

$$\frac{dy_4}{d\tau} = y_{04} + \sum_{n=1}^{5} p_{9,n} y_{4,n} + p_{15} y_5 - y_4(p_{14} y_3 y_4 + p_{13}),$$

$$\frac{dy_5}{d\tau} = p_{14} y_3 y_4 + \sum_{n=1}^{5} p_{6,n} y_{3,n} - y_5\left(\sum_{n=1}^{5} p_{5,n} y_{2,n} + p_{15}\right),$$

$$\frac{dy_6}{d\tau} = \frac{y_{06}(1 + p_{16})^h}{1 + (p_{17} y_L)^h} + \sum_{n=1}^{5} p_{8,n} y_{4,n} + \sum_{n=1}^{5} p_{9,n} y_{4,n} - y_6\left(\sum_{n=1}^{5} p_{7,n} y_{3,n} + p_{13}\right), \quad \text{(A.1)}$$

$$\frac{dy_{7,1}}{d\tau} = y_{07,1} + y_{6,1}(p_{11,1} + p_{12,1}) - y_{7,1}(p_{10,1} y_{5,1} + p_{13}),$$

$$\frac{dy_{7,2}}{d\tau} = y_{07,2} + p_{12,1} y_{6,1} - y_{7,2}(p_{10,2} y_{5,2} + p_{10,3} y_{5,3} + p_{13}),$$

$$\frac{dy_{7,3}}{d\tau} = y_{07,3} + y_{6,4}(p_{11,4} + p_{12,4}) - y_{7,3}(p_{10,4} y_{5,4} + p_{13}),$$

$$\frac{dy_{7,4}}{d\tau} = y_{07,4} + y_{6,5}(p_{11,5} + p_{12,5}) - y_{7,4}(p_{10,5} y_{5,5} + p_{13}),$$

$$\frac{dy_8}{d\tau} = p_{18} y_{10} + \sum_{n=1}^{5} p_{12,n} y_{6,n} - p_{19} y_8 y_9,$$

$$\frac{dy_9}{d\tau} = y_{09} + y_{10}(p_{18} + p_{20}) - y_9(p_{19} y_8 + p_{13}),$$

$$\frac{dy_{10}}{d\tau} = p_{19} y_8 y_9 - y_{10}(p_{18} + p_{20}),$$

Parameters of the model

Parameter	Value	Reference
k_1	5.2×10^7 M^{-1} min^{-1}	This paper
k_2, k_4, $k_{8,n}$, $k_{11,n}$, k_{13}, k_{15}, k_{18}, k_{22}, k_3	0.0116 min^{-1}	[23]
k_3	1.3×10^3 M^{-1} min^{-1}	This paper
$k_{5,1}$, $k_{5,2}$, $k_{5,4}$	1.4×10^8 M^{-1} min^{-1}	This paper
$k_{5,3}$, $k_{5,5}$	1.2×10^5 M^{-1} min^{-1}	This paper
$k_{6,1}$, $k_{6,2}$, $k_{6,4}$	0.221 min^{-1}	This paper
$k_{6,3}$, $k_{6,5}$	3.3×10^{-4} min^{-1}	This paper
$k_{7,1}$, $k_{7,2}$, $k_{7,4}$	4.9×10^3 M^{-1} min^{-1}	This paper
$k_{7,3}$, $k_{7,5}$	3.2×10^5 M^{-1} min^{-1}	This paper
$k_{9,n}$	1.4×10^{-4} min^{-1}	This paper
$k_{10,1}$	6.7×10^4 M^{-1} min^{-1}	This paper
$k_{10,2}$	2.4×10^4 M^{-1} min^{-1}	This paper
$k_{10,3}$	2.8×10^4 M^{-1} min^{-1}	This paper
$k_{10,4}$	1.4×10^4 M^{-1} min^{-1}	This paper
$k_{10,5}$	1.1×10^4 M^{-1} min^{-1}	This paper
$k_{12,1}$	0.255 min^{-1}	This paper
$k_{12,2}$	0.092 min^{-1}	This paper
$k_{12,3}$	2.2×10^{-4} min^{-1}	This paper
$k_{12,4}$	0.052 min^{-1}	This paper
$k_{12,5}$	8.7×10^{-5} min^{-1}	This paper
k_{14}	3.2×10^7 M^{-1} min^{-1}	This paper
k_{19}	3.9×10^7 M^{-1} min^{-1}	This paper
k_{20}	2.9 min^{-1}	This paper
k_{21}	1.8×10^6 M^{-1} min^{-1}	[35]
k_{23}	0.021 min^{-1}	[35]
γ	1.4×10^{-7} M	[13, 31]
h	2	[23]
X_{0L}	2.2×10^{-6} M	[36]
X_{01}	3.1×10^{-7} M	[37]
X_{02}	1.9×10^{-7} M	[37]
X_{03}	2.2×10^{-7} M	[37]
X_{06}	5.0×10^{-6} M	[38]
$X_{07,1}$	1.5×10^{-8} M	[39]
$X_{07,2}$	1.1×10^{-7} M	[39]
$X_{07,3}$	8.9×10^{-5} M	[31]
$X_{07,4}$	8.3×10^{-9} M	[40]
X_{09}	5.0×10^{-8} M	[41]
X_{012}	5.0×10^{-7} M	[42]
$\theta_{0,\,mutS}$	4	[4]
$\theta_{0,\,mutL}$	3.4	[4]
$\theta_{0,\,mutH}$	4.1	[4]
$\theta_{0,\,umu,\,mut}$	2.7	[4]
θ_1	10^{-9}	[33]
θ_2	3.31×10^{-2}	[34, 23]
$\theta_{3,\,mut+}$	2.72×10^{-9}	This paper
$\theta_{3,\,mutS}$	6.95×10^{-9}	This paper
$\theta_{3,\,mutL}$	4.9×10^{-9}	This paper
$\theta_{3,\,mutH}$	4.39×10^{-9}	This paper

$$\frac{dy_{11}}{d\tau} = p_{20}y_{10} + p_{22}y_{13} - p_{21}y_{11}y_{12},$$

$$\frac{dy_{12}}{d\tau} = y_{012} + y_{13}(p_{22} + p_{23}) - y_{12}(p_{21}y_{11} + p_{13}),$$

$$\frac{dy_{13}}{d\tau} = p_{21}y_{11}y_{12} - y_{13}(p_{22} + p_{23}),$$

$$\frac{dy_{14}}{d\tau} = p_{23}y_{13},$$

where $m = 1, ..., 4$ and $n = 1, ..., 5$.

The initial conditions for Eqs. (A.1) are the following: $y_{0,n}(0) = y_{00,n}$, $y_{1,n}(0) = 0$, $y_{2,n}(0) = 0$, $y_{3,n}(0) = 0$, $y_{4,n}(0) = 0$, $y_{5,n}(0) = 0$, $y_{6,n}(0) = 0$, $y_1(0) = y_{01}$, $y_2(0) = y_{02}$, $y_3(0) = y_{03}$, $y_4(0) = y_{04}$, $y_5(0) = 0$, $y_6(0) = y_{06}$, $y_{7,m}(0) = y_{07,m}$, $y_8(0) = 0$, $y_9(0) = y_{09}$, $y_{10}(0) = 0$, $y_{11}(0) = 0$, $y_{12}(0) = y_{012}$, $y_{13}(0) = 0$, $y_{14}(0) = 0$, where $m = 1, ..., 4$ and $n = 1, ..., 5$.

Here $y_{00,n}$, y_{01}, y_{02}, y_{03}, y_{04}, y_{06}, $y_{07,m}$, y_{09}, and y_{012} are the time-independent parameters representing the normalized initial concentrations of mismatches—$MutS_2$,$MutL_2$, MutH, GATCm, UvrD, exonucleases, PolIII, and DNA ligase, respectively. The initial levels of all the intermediate complexes are assumed to be zero at the beginning of repair. The normalization of the variables of the model is performed for the initial concentration of the MutS protein: $y_i = X_i/X_{01}$, and $y_{0i} = X_{0i}/X_{01}$. The values of the parameters X_{0i} for the MMR system in vivo are presented in the table.

Appendix B
PARAMETER VALUES

The dimensionless parameters of Eqs. (A.1) are $\tau = k_{13}t$, $p_1 = k_1X_{01}/k_{13}$, $p_2 = k_2/k_{13}$, $p_3 = k_3X_{01}/k_{13}$, $p_4 = k_4/k_{13}$, $p_{5,n} = k_{5,n}X_{01}/k_{13}$, $p_{6,n} = k_{6,n}/k_{13}$, $p_{7,n} = k_{7,n}X_{01}/k_{13}$, $p_{8,n} = k_{8,n}/k_{13}$, $p_{9,n} = k_{9,n}/k_{13}$, $p_{10,n} = k_{10,n}X_{01}/k_{13}$, $p_{11,n} = k_{11,n}/k_{13}$, $p_{12,n} = k_{12,n}/k_{13}$, $p_{13} = k_{13}/k_{13} = 1$, $p_{14} = k_{14}X_{01}/k_{13}$, $p_{15} = k_{15}/k_{13}$, $p_{16} = X_{0L}/\gamma$, $p_{17} = 1/\gamma$, $p_{18} = k_{18}/k_{13}$, $p_{19} = k_{19}X_{01}/k_{13}$, $p_{20} = k_{20}/k_{13}$, $p_{21} = k_{21}X_{01}/k_{13}$, $p_{22} = k_{22}/k_{13}$, and $p_{23} = k_{23}/k_{13}$. Here, t is the dimensional time; k_{13} is the rate constant of the nonspecific losses of the MMR proteins because of dilution due to bacterial growth; X_{01} is the basal level of the MutS protein in the cell in the absence of MMR-inducing lesions, and γ is the dissociation rate constant of the LexA monomer from the *UvrD* gene operator.

Most of the parameters k_j were determined by fitting the developed model to the in vitro experimental data on the MMR kinetics for the ExoI and RecJ pathways [27]. The fitting procedure is performed for a MutH-mediated incision, strand excision by exonucleases, and DNA resynthesis by PolIII. Each of these three stages was investigated for 3' and 5' DNA nick-

ing. The itted values for the parameters k_1, k_3, $k_{5,1} = k_{5,2} = k_{5,4}$, $k_{5,3} = k_{5,5}$, $k_{6,1} = k_{6,2} = k_{6,4}$, $k_{6,3} = k_{6,5}$, $k_{7,1} = k_{7,2} = k_{7,4}$, $k_{7,3} = k_{7,5}$, $k_{9,1} = k_{9,2} = k_{9,4}$, $k_{9,3} = k_{9,5}$, $k_{10,1}$, $k_{10,5}$, $k_{12,1}$, $k_{12,5}$, k_{14}, k_{19}, and k_{20} are presented in the Table. To obtain these parameters, we have set the initial conditions according to the reactant concentrations for in vitro reactions in [27]: $X_{00,1} = 2.4 \times 10^{-9}$ M, $X_{00,5} = 2.4 \times 10^{-9}$ M, $X_{01} = 3.7 \times 10^{-8}$ M, $X_{02} = 2.5 \times 10^{-8}$ M, $X_{03} = 1.0 \times 10^{-8}$ M, $X_{06} = 1.2 \times 10^{-8}$ M, $X_{07,1} = 1.8 \times 10^{-9}$ M, and $X_{07,4} = 7.8 \times 10^{-9}$ M. Since the number of GATCm sequences equals the total number of mismatches of all kinds, we set $X_{04} = X_{00,1} + X_{00,2} + X_{00,3} + X_{00,4} + X_{00,5}$. Wehave set the kinetic rates k_2, k_4, $k_{8,n}$, $k_{11,n}$, k_{13}, k_{15}, k_{18}, and k_{22} equal to zero because the experiment was performed in a constant reaction volume excluding the factor of cell culture growing. In Eqs. (A.1), we also omitted the following terms corresponding to the synthesis of the following MMR proteins: y_{01}, y_{02}, y_{03}, y_{04}, $y_{06}(1 + p_{16})h/(1 + (p_{17}y_L)^h)$, $y_{07,m}$, y_{09}, and y_{012}.

The parameters $k_{10,2}$, $k_{10,3}$, $k_{10,4}$, $k_{12,2}$, $k_{12,3}$, and $k_{12,4}$ are defined using $k_{10,1}$, $k_{10,5}$, $k_{12,1}$, and $k_{12,5}$ values and the relations between the turnover numbers of ExoI, RecJ and ExoVII, and ExoX. The exonuclease turnover numbers were taken from the experimental data: 6.9×10^3 nt/min (nucleotides per minute) for ExoI [28], 10^3 nt/min for RecJ [29], 2.5×10^3 nt/min for ExoVII [30], and 1.4×10^3 nt/min for ExoX [31]. The γ is assumed to be equal to the average value of the LexA dissociation rate from the SOS-box [13, 32]. The value of the Hill coefficient h is defined from the data on the binding cooperativity of the LexA repressor and UvrD regulatory region. As there is the only region of LexA binding to the UvrD operator [20], h is equal to 2 according to Aksenov et al. [23].

As was described before [13], the linear component of (3) characterizes the mutagenic lesions, which are fixed during constitutive repair or during DNA replication [7]. The mutagenic effectiveness can be defined by the DNA PolIII processing effectiveness. Therefore, according to [33], the coefficient of the linear component can be defined as $\theta_1 = 10^{-9}$.The value of the parameter θ_2, characterizing the number of pre-mutation lesions in an individual gene, is defined as follows. Since we use the *lacZ* gene for the analysis, let $L_1 = 3$, 075 base pairs be the length of the this gene, $L_0 = 4$, 639, 675 base pairs be the length of the whole *E. coli's* K-12 MG1655 genome [34], and $m_0 = 50$ J^{-1} m^2 is the yield of the pre-mutation lesions per full bacterial chromosome [23]. Then the average number of lesions in the *lacZ* gene is $L_1 m_0 \Psi / L_0 = \theta_2 \Psi$. Therefore, the proportionality coefficient is $\theta_2 = L_1 m_0 / L_0 = 3.31 \times 10^{-2}$.

Using the MMR model, it is possible to determine the coefficient 03 more precisely than in our previous study. The results obtained before indicated an ambiguous and complicated dependence of the resulting mutation frequency on the effectiveness of translesion synthesis. This fact was reflected in our SOS mutagenesis model by introducing the free parameter $p(X)$ describing the probability of wrong nucleotide insertion by the PolV Mut complex, which affects the θ_3 value. According to our previous calculations, $\theta_3 = L_1 k_s / L_0$, where k_s is the slope coefficient of a linear function characterizing the dependence of the mean number of the occurring errors on UV energy fluence. Simultaneous running of the models for SOS mutagenesis, translesion synthesis, and the MMR system for a *mut*$^+$ strain gives $k_s = 4.1 \times 10^{-6}$ under $p(X) = 6.1 \times 10^{-8}$ and, therefore, $\theta_3 = 2.7 \times 10^{-9}$. For *mut*$^-$ strains, these values are, respectively, the following: *mutS*$^-$, $k_s = 1.05 \times 10^{-5}$, $p(X) = 1.6 \times 10^{-7}$, θ_3, *mutS* $= 6.95 \times 10^{-9}$; *mutL*$^-$, $k_s = 7.4 \times 10^{-6}$, $p(X) = 1.1 \times 10^{-7}$, θ_3, *mutL* $= 4.9 \times 10^{-9}$; *mutH*$^-$, $k_s = 6.62 \times 10^{-6}$, $p(X) = 9.8 \times 10^{-8}$, θ_3, *mutH* $= 4.39 \times 10^{-9}$.

ACKNOWLEDGMENTS

This study was conducted as a part of the research project no. 301 "Mathematical Modelling of Genetic Regulatory Networks in Bacterial and Higher Eukaryotic Cells" between the Laboratory of Radiation Biology of Joint Institute for Nuclear Research and Cairo University. O. Chuluunbaatar acknowledges a financial support from the RFBR Grant no. 11-01-00523 and the JINR theme 09-6-1060-2005/2013 "Mathematical Support of Experimental and Theoretical Studies Conducted by JINR".

REFERENCES

1. R. S. Lahue, K. G. Au, and P. Modrich, Science **245**, 160–164 (1989); doi: 10.1126/science.2665076.
2. P. Modrich and R. Lahue, Annu. Rev. Biochem. **65**, 101–133 (1996); doi: 10.1146/annurev.bi.65.070196.000533.
3. G. M. Li, Cell Res. **18,** 85–98 (2008); doi: 10.1038/cr.2007.115.
4. L. Hongbo et al., Genetics **154**, 503–512 (2000).
5. L. M. Martin et al.,Cancer Treat. Rev. **36**, 518–527 (2010); doi: 10.1016/j.ctrv.2010.03.008.
6. M. Radman, "Phenomenology of an inducible mutagenic DNA repair pathway in *Escherichia coli*: SOS-repair hypothesis," in *Molecular and Environmental Aspects of Mutagenesis*, Ed. by L. Prakash et al. (Springfield, 1974), pp. 128–142.
7. E. M. Witkin, Bacteriol. Rev. **40**, 869–907 (1976).
8. E. A. Krasavin and C. Kozubek, Mutat. Res. **486**, 59–70 (2011); doi: 10.1016/S0921-8777(01)00089-1.
10. I. Yang et al., J. Biol. Chem. **278**, 13989–13994 (2003); doi: 10.1074/jbc.M212535200.
11. D. Chiapperino et al., J. Biol. Chem. **280**, 39684–39692 (2005); doi: 10.1074/jbc.M508008200.
12. M. Tang et al., Lett. Nat. **404**, 1014–1018 (2000); doi: 10.1038/35010020.

13. O. V. Belov, E. A. Krasavin, and A. Yu. Parkhomenko, J. Theor. Biol. **261**, 388–395 (2009); doi: 10.1016/j.jtbi.2009.08.016.
14. M. Radman and R. Wagner, Ann. Rev. Genet. **20**, 523–538 (1986); doi: 10.1146/annurev.ge.20.120186.002515.
15. S. W. Matson and A. B. Robertson, Nucl. Acids Res. **34**, 4089–4097 (2006); doi: 10.1093/nar/gkl450.
16. B. E. Dutra et al., Proc. Nat. Acad. Sci. USA **104**, 216–221 (2007); doi: 10.1073/pnas.0608293104.
17. A. Kornberg and T. A. Baker, *DNA Replication* (W. H. Freeman and Comp., N.Y., 1992).
18. O. V. Belov, E. A. Krasavin, and A. Yu. Parkhomenko, Part. Nucl., Lett. **6**, 260–273 (2009); doi: 10.1134/S1547477109030121.
19. O. V. Belov, E. A. Krasavin, and A.Yu. Parkhomenko, Biophysics **55**, 682–690 (2010); doi: 10.1134/S0006350910040287.
20. A. M. Easton and S. R. Kushner, Nucl. Acids Res. **11**, 8625–8640 (1983).
21. J. Courcelle et al., Genetics **158**, 41–64 (2001).
22. S. V. Aksenov, E. A. Krasavin, and A. A. Litvin, J. Theor. Biol. **186**, 251–260 (1997); doi: 10.1006/jtbi.1996.0353.
23. S. V. Aksenov, J. Biol. Phys. **25**, 263–277 (1999); doi: 10.1023/A:1005163310168.
24. Z. Livneh, J. Biol. Chem. **276**, 25639–25642 (2000); doi: 10.1074/jbc.R100019200.
25. V. G. Vaidyanathan B. P. Cho, Biochemistry **51**, 1983–1995 (2012); doi: 10.1021/bi2017443.
26. J. Malina et al., Chem. Asian J. **7**, 1026–1031 (2012); doi: 10.1002/asia.201100886.
27. A. Pluciennik et al., J. Biol. Chem. **284**, 32782–32791 (2009).
28. D. Lu et al., Biochemistry **48**, 6764–6771 (2009); doi: 10.1021/bi900361.
29. E. S. Han et al., Nucl. Acids Res. **34**, 1084–1091 (2006); doi: 10.1093/nar/gkj503.
30. A. A. Larrea et al., Nucl. Acids Res. **36**, 5992–6003 (2008); doi: 10.1093/nar/gkn588.
31. M. Viswanathan and S. T. Lovett, J. Biol. Chem. **274**, 30094–30100 (1999); doi: 10.1074/jbc.274.42.30094.
32. R. Mohana-Borges et al., J. Biol. Chem. **275**, 4708–4712 (2000); doi: 10.1074/jbc.275.7.4708.
33. J. W. Drake, Nature **221**, 1132 (1969); doi: 10.1038/2211133a0.
34. I. M. Keseler et al., EcoCyc: a comprehensive database of *Escherichia coli* biology," Nucl. Acids Res. **39**, D583–D590 (2011); doi: 10.1093/nar/gkq1143.
35. D. Georlette et al., Eur. J. Biochem. **267**, 3502–3512 (2000); doi: 10.1046/j.1432-1327.2000.01377.x.
36. D. Hegde et al., Mol. Gen. Gen. **246**, 254–258 (1995); doi: 10.1007/BF00294689.
37. G. Feng, H. C. Tsui, and M. E. Winkler, J. Bacteriol. **178**, 2388–2396 (1996).
38. M. A. Petit et al., Mol. Microbiol. **29**, 261–273 (1998); doi: 10.1046/j.1365-2958.1998.00927.x.
39. D. L. Cooper, R. S. Lahue, and P. Modrich, J. Biol. Chem. **268**, 11823–11829 (1993).
40. T. J. Haggerty and S. T. Lovett, J. Bacteriol. **179**, 6705–6713 (1997).
41. C. S. McHenry and A. Kornberg, J. Biol. Chem. **252**, 6478–6484.
42. E. C. Friedberg, G. C. Walker, and W. Siede, *DNA Repair and Mutagenesis* (ASM Press, D.C., Washington, 1995).